

Polymer Micelles with Hydrazone-Ester Dual Linkers for Tunable Release of Dexamethasone

Melissa D. Howard · Andrei Ponta · Allison Eckman · Michael Jay · Younsoo Bae

Received: 11 January 2011 / Accepted: 3 May 2011 / Published online: 26 May 2011
© Springer Science+Business Media, LLC 2011

ABSTRACT

Purpose To develop polymer micelles for the tunable release of Dexamethasone (DEX) in tumors.

Methods DEX was conjugated to poly(ethylene glycol)-poly(aspartate) block copolymers using hydrazone, ester, or hydrazone-ester dual linkers. Ketonic acids containing 3, 4, and 5 methylene groups were used as spacers to separate the dual linkers. Polymer micelles from the DEX-conjugated polymers were tested for drug release at different pH values and carboxylesterase activity levels.

Results DLS measurements and ¹H-NMR analysis confirmed all DEX-loaded micelles were < 100 nm with core-shell structure. Single linker micelles appeared unsuitable to release DEX preferentially in acidic tumor tissues. Hydrazone linkages between DEX and polymers were non-degradable at both pH 7.4 and 5.0. Ester linkages stable at pH 5.0 were unstable at pH 7.4. Hydrazone-ester dual linkers suppressed DEX release at pH 7.4 while accelerating drug release at pH 5.0. DEX release decreased at pH 5.0 as the length of ketonic acid increased but was independent of spacer length at pH 7.4. Dual linker micelles were stable in the presence of carboxylesterases, suggesting DEX release was primarily due to pH-dependent hydrolysis.

Conclusion Tunable release of DEX was achieved using pH-sensitive polymer micelles with hydrazone-ester dual linkers.

KEY WORDS dexamethasone · drug delivery · ester · hydrazone · polymer micelles

INTRODUCTION

Drug delivery using polymers has garnered significant attention in pharmaceutical research since polymer nanoassemblies were shown to carry various therapeutic agents to targeted disease sites in the body (1,2). Much recent work has focused on developing polymer drug carriers that release anticancer drugs in tumors in response to a biological stimulus (ions, pH or enzymatic activity) (3–6). However, techniques to control drug release patterns in a tunable way according to the disease states of cancer remain limited. Use of this novel drug delivery technique, dubbed ‘tunable release,’ would maximize anticancer efficacy by delivering drugs to tumors with the appropriate concentration and schedule (7). The design of drug-binding linkers becomes crucial to achieve this tunable drug release (8,9).

One of the emerging applications with tunable drug release is combination chemotherapy in order to overcome the resistance of cancer cells to single chemotherapeutic agents (10,11). Mechanisms for the resistant cancer cell survival are attributed to complicated intracellular pathways that can prevent anticancer drugs from reaching their therapeutic targets (12). Alternatively, cancer cells can enter a quiescent state to minimize the damage caused by chemotherapy (13). However, the use of multiple drugs can sensitize cancer cells when they are delivered with the appropriate concentrations, mixing ratios and therapeutic schedule (14). Currently, repetitive and sequential drug injections are the methods most frequently used for combination therapy. It is challenging

M. D. Howard · A. Ponta · A. Eckman · Y. Bae (✉)
Department of Pharmaceutical Sciences, College of Pharmacy
University of Kentucky
789 South Limestone
Lexington, KY 40536–0596, USA
e-mail: younsoo.bae@uky.edu

M. Jay
Division of Molecular Pharmaceutics, Eshelman School of Pharmacy
Lineberger Comprehensive Cancer Center
University of North Carolina at Chapel Hill
Chapel Hill, NC, USA

for these conventional methods to achieve optimal combination settings of multiple drugs in the body because each drug has a different pharmacokinetic profile (15). Tunable release would control not only the spatial but also temporal distribution of various drugs in tumors to supply drugs necessary for treatment with the right timing.

In addition to combination chemotherapy aimed at multiple therapeutic targets in cancer cells, the fibrous tissues and blood vessels in tumors can also be treated using tunable release. Such combination chemotherapy can modulate the tumor microenvironment to improve cancer chemotherapy further (16,17). The untreated tumor microenvironment is abnormal and heterogeneous (18). In a process known as the Warburg effect, cancer cells consume glucose inefficiently and produce a large amount of lactic acid that acidifies tumor tissues (19). The enhanced permeation and retention (EPR) effect demonstrates that tumors have leaky blood vessels and immature lymphatic drainage that allows for large molecules (< 500 nm) to permeate into and be retained in tumor tissues for a prolonged time (20). The Warburg and EPR effects are rationales for pH-sensitive drug carriers that can deliver and release drugs preferentially in tumor tissues. Accumulated results suggest that even though tumor-preferential drug delivery is achieved successfully, it is still difficult for drugs to penetrate into tumors due to the irregular blood supply, thick fibrosis, elevated interstitial fluid pressure (IFP) and hypoxia of tumors (21,22). Therefore, tunable release may allow combination therapy to change the tumor microenvironment and inhibit cancer cells concurrently or sequentially.

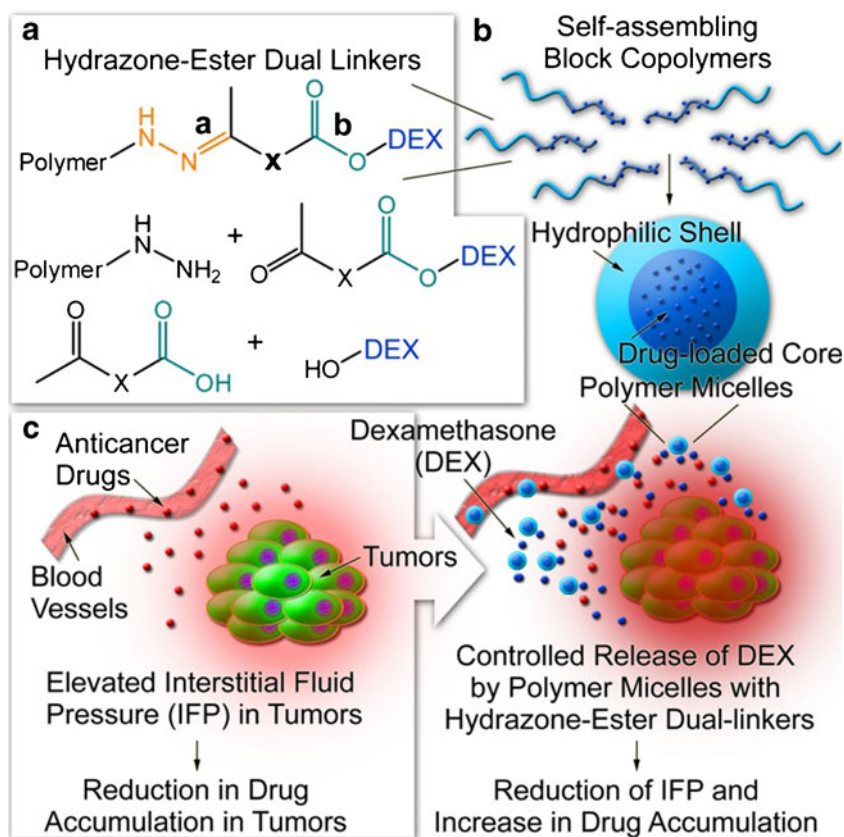
Dexamethasone (DEX) is an anti-inflammatory agent that can be used to reduce the IFP of tumors (23,24). Previous studies showed that pretreatment with DEX reduced the IFP and enhanced the accumulation of chemotherapeutic agents in tumors (25,26). Although the results suggest a promising combination therapeutic approach, DEX is limited in clinical applications due to immunosuppressive side effects after systemic administration (27,28). Currently, there is no facile and effective way to achieve tunable release of DEX avoiding complicated chemistry. Previously developed delivery systems for DEX have relied on linker chemistry using degradable linkers (hydrazone or ester) to conjugate DEX to water-soluble polymers at its ketone (C3 and C20) (29,30) or hydroxyl (C21) moieties (31,32). Their DEX release patterns were either too slow or too fast to achieve tumor preferential delivery of DEX. In order to minimize the side effects and maximize the combination effects of DEX with other drugs, drug carriers should retain DEX stably in the blood and release the drug in

tumor tissues for a period of time long enough to reduce the IFP of tumors. We think that dual linkers comprised of hydrazone and ester bonds would be a useful tool to resolve these issues, taking advantage of their acid-labile and enzymatically degradable properties in combination (33).

In addition to the linker chemistry, a drug delivery platform is another important factor necessary to achieve tumor-preferential tunable release. Polymer drug carriers show different distribution patterns in the body (biodistribution), depending on the particle size, shape, and surface properties (2,34–37). The effect of carriers on the biodistribution should be minimized to predict the tumor-preferential delivery of drugs correctly (38). The most efficient and effective way to minimize the variable carrier effect is to entrap drugs and linkers inside drug carriers (39,40). For these reasons, we used polymer micelle drug carriers in this study. Polymer micelles are spherical polymer nanoassemblies with a distinctive core-shell structure. Polymer micelles have been touted as promising drug carriers because they can protect drug payloads from the *in vivo* environment by entrapping drugs in a hydrophobic core enveloped by a hydrophilic shell (41). Several preclinical and clinical studies have shown that polymer micelles improve the bioavailability and tumor-targeted delivery of various therapeutic agents while allowing chemical modifications to the core and shell for multifunctional applications (42). We have shown that polymer micelles from poly(ethylene glycol)-poly(amino acid) block copolymers are a versatile drug delivery platform to design multifunctional drug carriers (43).

In this study, we prepared polymer micelles that entrap DEX through hydrazone-ester dual linkers to achieve pH-controlled drug release in a tunable manner (Fig. 1a). The dual linkers consist of acid-labile hydrazone (a) and enzymatically degradable ester (b) linkages, while spacers (X) modulate DEX release patterns and stability of the micelles. The dual linker micelles can achieve tunable release of DEX in tumors (Fig. 1b), reducing the IFP that limits tumor accumulation of other drugs (Fig. 1c). Micelles with single hydrazone or ester linkers were also tested for acid-sensitive DEX release. The physicochemical properties of the micelles, including particle size and DEX release patterns, were characterized at different pH values corresponding to the normal physiological condition (pH 7.4) and the acidic tumor tissues (pH 5.0). Stability of DEX-loaded micelles was also tested in the presence of carboxylesterase, a digestive enzyme of ester bonds. Our characterization of the DEX-loaded polymer micelles provides valuable insight into the design of drug-binding linkers and drug carriers for tunable release.

Fig. 1 Mechanism of tumor-preferential tunable release of DEX from polymer micelles. Polymer micelles entrap DEX through hydrazone-ester dual linkers (**a**). The dual linkers consist of acid-labile hydrazone linkages (**a**) and enzymatically degradable ester linkages (**b**), while spacers (X) modulate DEX release patterns and stability of the micelles. The dual linker micelles can achieve tunable release of DEX in tumors (**b**), reducing the IFP that limits tumor accumulation of other drugs (**c**).



MATERIALS AND METHODS

Materials

α -Methoxy- ω -amino poly(ethylene glycol) (PEG-NH₂, MW = 12,266) was purchased from NOF Corporation (Japan). L-aspartic acid β -benzyl ester, triphosgene, 4,4-diphenyl-cyclohexa-2,5-dienone, 2-hydroxy-1-(1-hydroxycyclohexyl)ethanone, 4-acetylbutyric acid (ABA), 6-oxoheptanoic acid (OHA), 7-oxooctanoic acid (OOA), dexamethasone (DEX), prednisolone, N,N'-diisopropylcarbodiimide (DIC), 4-(dimethylamino)pyridine (DMAP), acetonitrile (ACN), benzene, N,N-dimethylformamide, anhydrous N,N-dimethylformamide (DMF), anhydrous dimethylsulfoxide (DMSO), dimethylsulfoxide-d₆ (DMSO-*d*₆), deuterium oxide (D₂O), anhydrous ethyl ether, anhydrous hexane, anhydrous hydrazine, anhydrous tetrahydrofuran (THF), acetate buffer solution, and phosphate buffer solution were purchased from Sigma-Aldrich (USA). Regenerated cellulose dialysis bags with molecular weight cut-off (MWCO 6–8,000 Da) and Slide-A-Lyzer G2 dialysis cassettes with MWCO 10,000 were purchased from Fisher Scientific (USA). Amicon-Ultra centrifugal ultrafiltration devices with MWCO 10,000 were purchased from Millipore (USA).

PEG-PBLA Block Copolymer Synthesis

Our synthesis protocol is shown in Fig. 2. β -Benzyl-L-aspartate N-carboxy anhydride (BLA-NCA, **2**) was prepared using the Fuchs-Farthing method as described elsewhere (39). Triphosgene (2.88 g, 9.7 mmol) and β -benzyl-L-aspartate (5.0 g, 22.4 mmol) were mixed in dry THF (100 mL). The reaction was conducted in N₂ at 45°C until the solution turned clear. Anhydrous hexane was slowly added to the reaction solution for recrystallization of BLA-NCA in -20°C. Purified BLA-NCA was polymerized in anhydrous DMSO at 45°C for 2 days by using amino-terminated PEG as a macroinitiator. The amount of BLA-NCA was adjusted with respect to PEG to prepare PEG-PBLA block copolymers with 35 units of aspartic acid, **3**. The reaction solution was precipitated in anhydrous ethyl ether. White PEG-PBLA was collected by freeze-drying from benzene.

PEG-p(Asp-Est-Dex) Synthesis

PEG-PBLA was dissolved in 0.1 N NaOH to deprotect benzyl ester groups. The solution was dialyzed against deionized water using MWCO 6–8,000 Da until NaOH

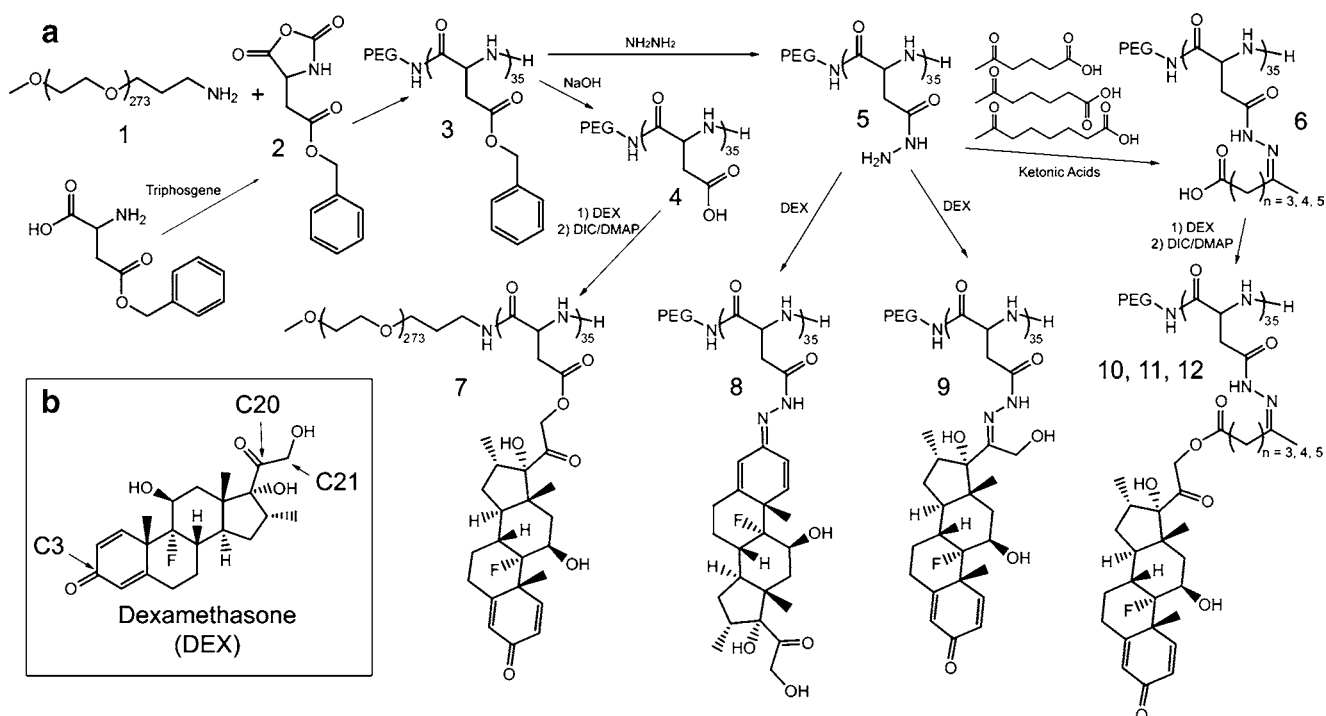


Fig. 2 (a) Synthesis of block copolymers. PEG-PBLA, **3**, was prepared from 12 kDa PEG, **1**, and 35 units of BLA-NCA, **2**. PEG-p(Asp), **4**, was produced by complete deprotection of **3** in 0.1 N NaOH. DEX was conjugated to **4** through an ester linkage by an esterification reaction between the hydroxyl group at the C21 moiety of DEX and carboxyl groups of **4** to give **7**. DEX was conjugated at its C3 and C20 positions to PEG-p(Asp-Hyd), **5**, through ketone linkages to produce **8** and **9**, respectively. Reactions between **5** and various ketonic acids (ABA, OHA, and OOA) produced **6**, in which the ketonic acids served as spacers. DEX was conjugated to **6** through an esterification reaction to give three polymer compositions with hydrazone-ester dual linkers (**10–12**). (b) Structure of DEX.

was removed completely. PEG-poly(aspartate) [PEG-p(Asp), **4**] was collected by freeze-drying. DEX was conjugated to PEG-p(Asp) through an ester bond in DMSO at room temperature. DIC and DMAP were used for the esterification reaction. The reaction solution was precipitated in anhydrous ethyl ether. The product was freeze-dried from benzene to collect PEG-poly(aspartate ester dexamethasone) [PEG-p(Asp-Est-DEX), **7**]. Sample aliquots were filled with nitrogen to minimize hydrolytic degradation.

PEG-p(Asp-Hyd-DEX) Synthesis

Hydrazide groups were introduced to PEG-PBLA through aminolysis reactions as previously reported (44). PEG-PBLA and anhydrous hydrazine were reacted in DMSO at 45°C for 1 h (50–100 mg polymer/ml DMSO) to prepare PEG-poly(aspartate hydrazide) [PEG-p(Asp-Hyd), **5**]. PEG-p(Asp-Hyd) was precipitated in anhydrous ethyl ether and freeze-dried from benzene. DEX and PEG-p(Asp-Hyd) were mixed in DMSO at 40°C for 72 h. The reaction solution was precipitated in anhydrous ethyl ether repeatedly. The precipitates were collected from benzene to

provide PEG-poly(aspartate hydrazide dexamethasone) [PEG-p(Asp-Hyd-DEX), **8** and **9**].

PEG-p(Asp-Hyd-X-Est-DEX) Synthesis ('X' Indicates Ketonic Acids as Spacers)

PEG-p(Asp-Hyd) block copolymers were reacted with three ketonic acids (ABA, OHA and OOA) separately in DMSO at 40°C for 3 days. Reaction solutions were precipitated in anhydrous ethyl ether, followed by freeze-drying from benzene. Each PEG-p(Asp-Hyd) modified with ketonic acids, **6**, was reacted with DEX in DMSO at room temperature by adding DIC and DMAP. The reactions were conducted for 24 h, followed by precipitation in anhydrous ethyl ether and freeze-drying from benzene. The ketonic acids provided spacers of 3, 4 and 5 methylene groups ('X') between PEG-p(Asp-Hyd) and DEX in the final products [PEG-p(Asp-Hyd-X-Est-DEX), **10**, **11** and **12**].

Polymer Micelle Preparation

Polymer micelles were prepared from **7**, **8**, **9**, **10**, **11** and **12**. Either reconstitution or freeze-drying methods were

used to prepare the micelles. The reconstitution method was conducted by dissolving drug-conjugated polymer powders directly in aqueous solutions and sonicating the solution. For the freeze-drying method, block copolymers were dissolved in ACN first and diluted with deionized water, adjusting the final ACN content to 20%. The block copolymer solutions were freeze-dried, following dry ice freezing. Freeze-dried micelle powders were reconstituted in aqueous solutions. All micelles were filtered through 0.22 μm filters prior to further experiments. Polymer micelles from DEX-conjugated block copolymers are abbreviated according to the drug-binding linkers used, which include hydrazone (HYD-M), ester (EST-M), hydrazone-ABA-ester (ABA-M), hydrazone-OHA-ester (OHA-M) and hydrazone-OOA-ester (OOA-M).

Analytical Methods

Particle size of polymeric micelles in water was determined by dynamic light scattering (DLS) measurements using a Zetasizer Nano-ZS (Malvern, UK). The instrument was equipped with a He-Ne laser (4 mW, 633 nm) and set up to collect 173° angle scattered light. Number distributions are presented as the mean particle size. $^1\text{H-NMR}$ experiments were performed on a Varian 500 MHz NMR (Varian Inc., Palo Alto, CA) at 25°C. Products were dissolved in DMSO-*d*₆ and analyzed following each step in the synthetic pathway. NMR spectra were also obtained for freeze-dried micelles reconstituted in D₂O. Where appropriate, gel permeation chromatography (GPC) was additionally used to confirm the success of reactions. The system was a Shimadzu Prominence HPLC series equipped with a Shodex Asahipack GF-7 M HQ column and an RID-10A refractive index detector. The mobile phase was 5 mM PBS run at 0.5 ml/min; the column temperature was held at 35°C. Molecular weight was calculated through comparison with a calibration curve based on PEG standards. The polydispersity index was calculated by dividing the weight average molecular weight by the number average molecular weight. DEX loading was confirmed by $^1\text{H-NMR}$ and quantified by HPLC. Ester-containing micelles were prepared at 2 mg/ml in either acetate buffer (10 mM pH 5.0, $n=3$) or phosphate buffer (10 mM pH 7.4, $n=3$). One hundred μL of each sample were combined with 100 μL prednisolone (0.1 mg/ml) as an internal standard and 10 μL NaOH (0.1 N). The mixed solutions were incubated at 37°C overnight with shaking at 100 rpm. Samples were neutralized with 10 μL HCl (0.1 N). One hundred μL of neutralized samples were mixed with ACN (45% ACN/55% H₂O) and ultrafiltered. Filtrates were analyzed by HPLC according to the following conditions. The system was a Shimadzu Prominence HPLC series equipped with a SPD-M20A Photodiode Array Detector. Five- μL samples

were injected to an Eclipse XDB-C18 (4.6 mm \times 150 mm, 5 micron, Agilent Technologies) column at 40°C. The mobile phase (45% ACN/55% H₂O) was run at a flow rate of 1 ml/min. Concentrations were calculated based on peak area calibration curves prepared for DEX and Prednisolone at 254 nm from 1 to 500 $\mu\text{g/ml}$.

pH-Dependent Drug Release Study

Drug release studies were conducted in acetate (10 mM, pH 5.0) and phosphate (10 mM, pH 7.4) buffers under sink conditions. Samples were removed at 0 h from initial preparations. Dialysis cassettes were loaded with 400 μL of 2 mg/ml micelle solutions and placed into 5 L of buffer solutions at 37°C. At each time point (1, 3, 6, and 24 h), the entire internal solution was collected from three dialysis cassettes and stored at room temperature until all samples had been collected. Samples were treated as described above to determine drug loading by HPLC analysis. Data are presented as percent drug remaining, using 0 h concentrations as the standard. The area under the curve (AUC_{0-t}, where 't' represents a time point) was determined by using the trapezoidal rule for % DEX released (% DEX released = 100% DEX remaining) with respect to time. We compared AUC values for the early (0–3 h) and late (3–24 h) periods.

Carboxylesterase-Dependent Drug Release Study

Polymer micelles (2 mg/ml) were incubated under non-sink conditions at 37°C/pH 7.4 in media with varying levels of carboxylesterase (CE) activity: 1) RPMI cell culture medium, 2) RPMI with 10% fetal bovine serum (FBS), 3) RPMI with 10% mouse plasma (MP), 4) RPMI with 10% human plasma (HP), 5) RPMI with 10% FBS and 10% MP, and 6) RPMI with 10% FBS and 10% HP. Mouse plasma is known to have higher levels of CE activity than human plasma (45). RPMI was used as a control to determine the effects of ions and small molecules (vitamins and amino acids) on micelle stability. FBS was used as a control for general protein effects on micelle stability. All combinations were prepared on a volume basis. Plasma samples contained sodium heparin as the anti-coagulant. One hundred μL aliquots ($n=3$) were collected at 0 and 24 h, followed by ultrafiltration and HPLC analysis as described above. Drug release patterns were determined by quantifying cleaved DEX and DEX-ketonic acid conjugates.

Statistics

Statistical analyses were performed using ANOVA (single factor) at the 5% significance level. Data were recorded as

mean \pm standard deviation. All experiments were done in triplicate as specified in the results section. Data analyses were performed using Microsoft Excel (2007).

RESULTS

Block Copolymer Synthesis

Figure 2 summarizes the synthetic pathways for all materials used in the research. Using the PEG peak as a reference, $^1\text{H-NMR}$ indicated that the polymerization reaction between 12 kDa PEG, **1**, and BLA-NCA, **2**, had proceeded to give PEG-PBLA, **3**, with 35 units of aspartic acid. GPC further showed neither unreacted PEG nor PBLA homopolymers after purification. Molecular weight distribution of the block copolymers was homogeneous with a polydispersity index smaller than 1.3. The results were consistent with what we observed previously. PEG-p(Asp), **4**, was produced by complete deprotection of **3** in 0.1 N NaOH. DEX was conjugated to **4** through an ester linkage by an esterification reaction between the hydroxyl group at the C21 moiety of DEX and carboxyl groups of **4** to give **7**. DEX loading was 8.67 ± 0.86 wt% ($n=6$). DEX was conjugated at its C3 and C20 positions to PEG-p(Asp-Hyd), **5**, through ketone linkages to produce **8** and **9**, respectively. Drug loading for these two products together appeared low by $^1\text{H-NMR}$ and could not be quantified by HPLC due to difficulties in cleaving the drug from the polymer. Reactions between **5** and various ketonic acids (ABA, OHA, and OOA) produced **6** in which the ketonic acids served as spacers containing 3, 4 and 5 methylene groups. DEX was subsequently conjugated to **6** through esterification to give three polymer compositions with hydrazone-ester dual linkers, **10**, **11**, and **12**. DEX loadings were 4.63 ± 0.75 , 5.57 ± 0.61 , and 4.50 ± 0.28 wt% for **10**, **11**, and **12**, respectively ($n=6$).

Polymer Micelle Preparation

All DEX-conjugated block copolymers formed polymer micelles irrespective of the composition. Freeze-dried micelles were readily reconstituted in aqueous solutions at concentrations >2 mg/ml; no precipitate was observed. Prepared micelles were smaller than 100 nm: EST-M (85.74 nm), ABA-M (61.50 nm), OHA-M (43.82 nm), and OOA-M (37.84 nm). $^1\text{H-NMR}$ spectra of the micelles in DMSO-*d*₆ (Fig. 3) showed the characteristic peaks of DEX (dienone (7.3, 6.2 and 6.0 ppm) and hydroxyethanone (5.2 ppm)) and PEG (3.5 ppm). A complete reduction of DEX peaks was seen in the micellar spectra in D₂O, while the PEG peak remained, indicating that DEX is primarily entrapped within the micelles.

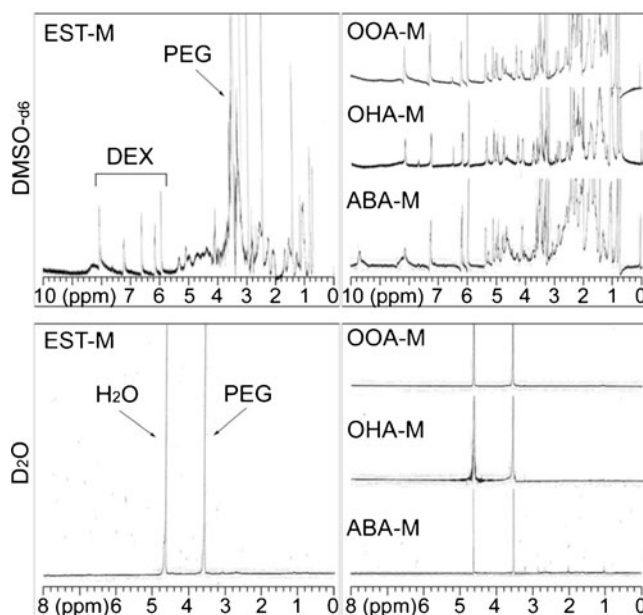
HYD-M, a mixture of **8** and **9**, did not form homogeneous polymer micelles. We were unable to determine the particle size of HYD-M because it varied between batches (4.50–2187.20 nm). Our preliminary experiments showed that drug release from HYD-M (**8,9**) was negligible even under strongly acidic conditions (pH <2) and at elevated temperatures ($> 60^\circ\text{C}$). To elucidate the mechanism, PEG-p(Asp-Hyd) was reacted with two model ketone compounds, 4,4-diphenyl-cyclohexa-2,5-dienone and 2-hydroxy-1-(1-hydroxycyclohexyl) ethanone, which represent the C3 and C20 moieties of DEX, respectively. HPLC analysis revealed that hydrazone formation at the C3 ketone of DEX is favorable and highly stable compared to the hydrazone at the C20 ketone of DEX. Based on these results, we concluded that direct conjugation of DEX to PEG-p(Asp) through the hydrazone would be inappropriate to design our polymer micelles for the delivery and pH-sensitive release of DEX in tumors. We did not pursue further experiments with HYD-M accordingly.

pH-Dependent DEX Release from the Micelles

Drug release patterns showed that EST-M was unstable at pH 7.4, while it was more stable at pH 5.0 (Fig. 4). 51.39% and 32.37% of DEX were released from EST-M in 6 h at pH 7.4 and pH 5.0, respectively. Polymer micelles with hydrazone-ester dual linkers showed the opposite drug release patterns. In all cases (ABA-M, OHA-M, and OOA-M), DEX release from the micelles was suppressed at pH 7.4 and accelerated at pH 5.0. The results suggest that polymer micelles with hydrazone-ester dual linkers may remain stable in blood and release more DEX in acidic tumor tissues. DEX release was reduced at pH 5.0 as the chain length of the spacer increased. Interestingly, DEX release was less dependent on the spacer at pH 7.4. To suppress DEX release at pH 7.4, we also attempted to test ketonic acids longer than OOA, but the block copolymers precipitated forming no micelles (data not shown).

We compared DEX release profiles by calculating the AUC values of DEX released at different pH conditions. Data were analyzed by separating the AUC values for the early (0–3 h) and late (3–24 h) time periods (Table I). The AUC₀₋₃ showed that ABA-M suppressed drug release at pH 7.4 effectively with respect to EST-M. OHA-M and OOA-M released slightly more drugs than EST-M in the same time period. At pH 5.0 (0–3 h), all micelles released DEX in a pH-dependent manner. At later time periods (AUC₃₋₂₄), DEX release at pH 7.4 was slower and more sustained in all micelles with dual linkers compared to EST-M. The AUC₃₋₂₄ at pH 5.0 showed that ABA-M released more DEX than either OHA-M or OOA-M. It is intriguing that OOA-M, containing longer and more hydrophobic spacers,

Fig. 3 $^1\text{H-NMR}$ spectra of polymer micelles in $\text{DMSO-}d_6$ and D_2O . $^1\text{H-NMR}$ spectra of the micelles in $\text{DMSO-}d_6$ showed the characteristic peaks of DEX (dieneone (7.3, 6.2 and 6.0 ppm) and hydroxyethanone (5.2 ppm)) and PEG (3.5 ppm). A complete reduction of DEX peaks was seen in the micellar spectra in D_2O while the PEG peak remained, indicating that DEX was entrapped within the micelles.



released more DEX than OHA-M. Among the micelles with dual linkers, ABA-M released the least amount of DEX at pH 7.4 and the greatest amount of drug at pH 5.0 during the early time period (0–3 h). In the later time period (3–24 h), all micelles showed similar DEX release patterns at pH 7.4. However, ABA-M still released more DEX than OHA-M and OOA-M at pH 5.0. Based on the

pH-dependent drug release studies, ABA-M was chosen as the lead composition for further studies.

Carboxylesterase-Dependent Drug Release

In addition to pH, we tested stability of ABA-M in the presence of carboxylesterase (CE) to confirm that polymer

Fig. 4 Time- and pH-dependent release of DEX from polymer micelles at 37°C . EST-M was unstable at pH 7.4, while it was more stable at pH 5.0. Polymer micelles with hydrazone-ester dual linkers showed the opposite drug release patterns with drug release being accelerated at pH 5.0 and suppressed at pH 7.4. DEX release was reduced at pH 5.0 as the chain length of the spacer increased but was less dependent on the spacer at pH 7.4.

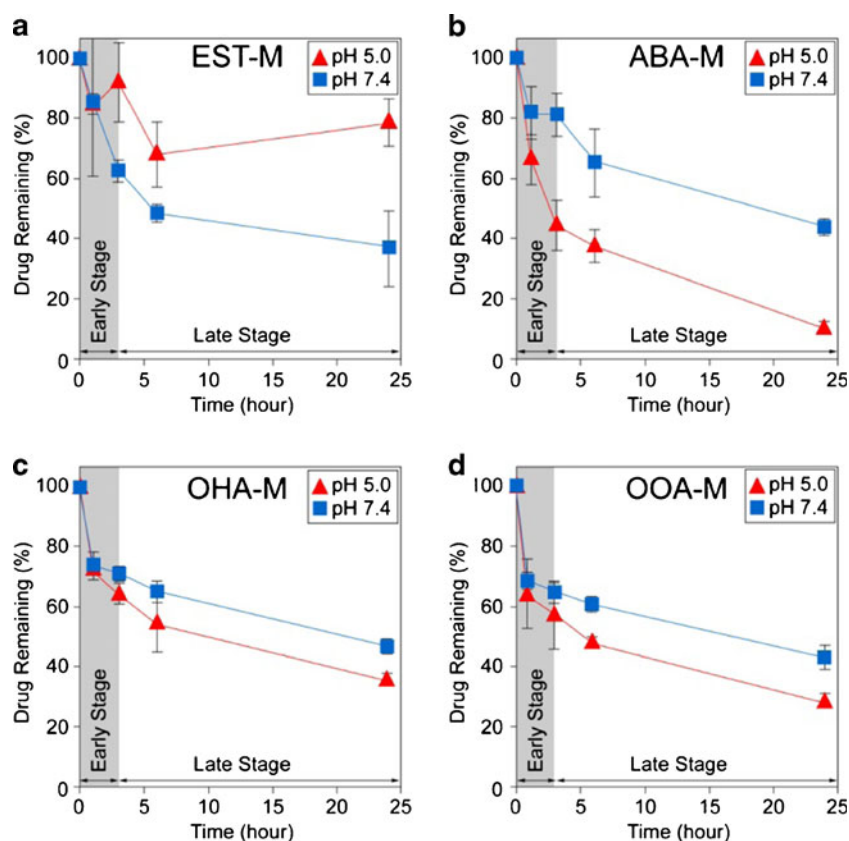


Table 1 Accumulated DEX Release from Polymer Micelles

	pH	Micelles	AUC ^a		Micelles/EST-M ^c		Micelles/ABA-M ^c	
			% DEX released × hour ^b		0–3 h	3–24 h	0–3 h	3–24 h
			0–3 h	3–24 h	0–3 h	3–24 h	0–3 h	3–24 h
7.4		EST-M	59.62	1162.83	1	1	–	–
		ABA-M	45.20	893.03	0.76	0.77	1	1
		OHA-M	70.02	893.24	1.17	0.77	1.55	1.00
		OOA-M	83.86	983.39	1.41	0.85	1.86	1.10
5.0		EST-M	30.29	540.59	1	1	–	–
		ABA-M	105.38	1536.74	3.48	2.84	1	1
		OHA-M	76.27	1106.28	2.52	2.05	0.72	0.72
		OOA-M	97.17	1254.63	3.21	2.32	0.92	0.82

^aAUC denotes the area under the curve of DEX released from the micelles.

^bThe unit for AUC is defined as % DEX release × hour.

^cThe ratios show DEX released from each micelle with respect to either EST-M or ABA-M.

micelles can protect DEX and the ester linkers from enzymatic degradation. The micelles were incubated at 37°C under six different conditions as described in the Materials and Methods section. Total DEX released from ABA-M is summarized in Fig. 5. No dissociation of micelles was seen in all incubation conditions at 0 h. DEX release was minimal (< 5%) at the initial time point. An ANOVA analysis indicated no significant differences among the six samples at 0 h ($P > 0.05$). It is noticeable that ABA-M remained stable in RPMI, FBS, MP and HP alone or in combination, suggesting that the micelles protected DEX and the dual linkers in the solutions that contain various additives such as ions, small molecules, amino acids, proteins and digestive enzymes. Following 24 h incubations, DEX release was slightly higher (10–15%) in samples containing mouse plasma compared to the samples lacking CE activity ($P < 0.05$). A slight difference in release was also observed between drug release in this study and the pH-dependent study described above, which may be attributable to the non-sink *versus* sink conditions employed.

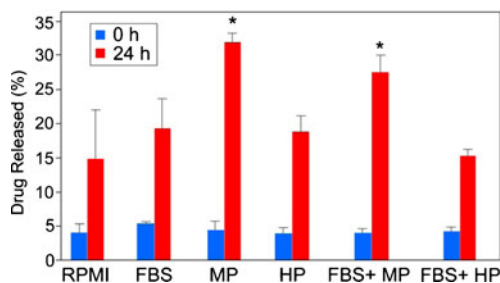


Fig. 5 Stability of polymer micelles (ABA-M) in cell culture medium (RPMI), 10% fetal bovine serum (FBS), 10% mouse plasma (MP), 10% human plasma (HP), and in combinations of these. Drug release was low at the initial time point, indicating that polymer micelles are stable in the presence of biological media. Drug release was slightly elevated in media containing CE at 24 h as compared to media lacking CE ($p < 0.05$, denoted by *).

DISCUSSION

We previously reported that polymer micelles comprised of PEG-p(Asp) block copolymers are versatile drug carriers for controlled delivery of various drugs to tumors (43). Tumor-preferential delivery of DEX using the polymer micelles is expected to reduce the interstitial fluid pressure of tumor tissues while suppressing the systemic toxicity of the drug. In comparison to other delivery approaches, we anticipate that the polymer micelles prepared in this study would minimize the effect of chemical modification on the pharmacokinetic profiles of drug carriers while still achieving pH-dependent release of DEX in tumors. Prompt and sustained release of DEX in tumors may be achievable using micelles capable of tunable release.

Polymer Synthesis and DEX Conjugation

DEX was conjugated to PEG-p(Asp) block copolymers through hydrazone-ester dual linkers to prepare polymer micelles that can release the drug preferentially in acidic tumor tissues ($pH < 7.0$). We initially tested DEX conjugation to PEG-p(Asp-Hyd) block copolymers using single hydrazone and ester linkers. While DEX could be conjugated to block copolymers directly through a hydrazone linker, the drug loading was low and the hydrazone bond appeared too stable to release the drug in a physiologically relevant time period. Further, micelles from this composition were not homogenous in size, which may result from both **8** and **9** being present or from the polymers having an insufficiently hydrophobic section due to the low drug load. The results also indicated that DEX conjugation through ester linkers had limited stability. Polymer micelles entrapping DEX through ester would be unsuitable for drug delivery to tumors because more drugs would be released in blood ($pH 7.4$) than in acidic tumor tissues ($pH < 7.0$). In spite of these apparent failures at

achieving pH-dependent DEX release, each linkage still showed successful reaction yields (hydrazone formation) and high drug conjugation (ester formation) between DEX and block copolymers. To take advantage of these possibilities, DEX was conjugated to the block copolymers using a hydrazone-ester dual linker with ketonic acids of varying carbon chain lengths introduced as spacers. DEX loading (4.50–5.57 wt%) was high enough to prepare polymer micelles that can carry the drug at concentrations even greater than the effective dose (< 1 mg/kg) (46) for future *in vivo* applications.

Preparation of DEX-Loaded Micelles

Block copolymers with hydrazone-ester dual linkers formed polymer micelles smaller than 100 nm, which is clinically relevant for tumor preferential drug delivery by the EPR effect (47). Interestingly, particle size of the micelles with dual linkers decreased as hydrophobicity of ketonic acids increased in comparison to EST-M. This may be attributable to how the different polymer compositions assemble into micelles with differences in hydrophobicity leading to a change in the micellar aggregation number. ¹H-NMR analysis in DMSO-*d*₆ confirmed DEX conjugation to polymers (Fig. 3). The NMR spectra of the micelles in D₂O showed a complete reduction of peaks from free DEX and the core-forming segment of PEG-p(Asp) block copolymers. Only the PEG peak was observed in all micelle compositions. These results indicate that micelles exhibited the expected core-shell structures with PEG on the surface and the hydrophobic portion of the polymers forming the core to which DEX was entrapped with limited molecular mobility. It is noted that polymer micelles were readily prepared by reconstituting freeze-dried powders, which would facilitate the pharmaceutical development of DEX-loaded polymer micelles.

pH-Dependent DEX Release from the Micelles

Polymer micelles with hydrazone or ester single linkers were unsuitable to achieve DEX release in the acidic environment of tumors. The hydrazone linker was too stable to release DEX in both pH 7.4 and 5.0 solutions, likely as a result of the multiple double bonds present around the hydrolytic site when DEX is conjugated at the C3 position. DEX release from HYD-M was negligible in 72 h. Similar results have been observed previously. Hydrazone bonds based on aromatic aldehydes have been shown to display enhanced stability under acidic conditions over those based on aliphatic aldehydes (48,49). This was attributed to the conjugation of the π bonds of the $-C=N-$ bond of the hydrazone with the π -bonding benzene ring, and it can be assumed that similar factors are at play in this system. Ester

linkers caused undesirable DEX release from the micelles at pH 7.4 while suppressing drug release at pH 5.0. *In vivo* applications of our polymer micelles with single linkers appeared unlikely for parenteral delivery of DEX. Ester linker micelles may alternatively be suitable for oral delivery of DEX, as they may remain stable in acidic gastric fluids until they reach the small intestine.

Polymer micelles with hydrazone-ester dual linkers achieved DEX release suitable for tumor-preferential delivery of DEX. As DEX is conjugated to these polymers following the insertion of a spacer, the hydrazone linker regains its susceptibility to pH-dependent hydrolysis that was lost in the HYD-M composition. In comparison to EST-M, the dual linker micelles suppressed DEX release at pH 7.4 while accelerating DEX release at pH 5.0. Similarly to the hydrazone linker, the difference in ester stability between the single and dual linkers can be attributed to the surrounding chemical structure. Previous studies have shown that an increase in the carbon chain length of ester side chains slows hydrolysis (50,51), which is observed in comparing EST-M with the dual linker micelles. This may be partially attributable to steric hindrance issues or to the fact that the carbon chains serve as electron donating groups, decreasing the susceptibility of the bond to attack. Importantly, the results suggest that polymer micelles with dual-linkers will remain stable in blood and release more DEX in acidic tumor tissues. DEX release at pH 5.0 was dependent on the chain length of ketonic acid spacers for the dual linker micelles. DEX remaining in OHA-M and OOA-M at 24 h were greater than ABA-M. The suppressed drug release at pH 5.0 with longer ketonic acids may be attributed to the increased hydrophobicity stabilizing the micelle core. The difference in DEX release between OHA-M and OOA-M was not significant. There was no difference in DEX release at pH 7.4, irrespective of the spacer length. These results suggest that the hydrazone is responsible for drug release at pH 5.0, while ester hydrolysis contributes to DEX release at pH 7.4.

It is unknown why polymer micelles did not prevent linkers from hydrolysis at pH 7.4. Our initial expectation was that more hydrophobic spacers would make the micelle cores more stable and thus suppress drug release further. However, even though DEX molecules are tightly entrapped in the micelle core (as seen in the ¹H-NMR analysis), the polymer micelle cores may be porous enough to allow water molecules to penetrate and attack both bonds. Previous results have shown that hydrolysis of small molecule prodrugs with ester linkages can be suppressed as the chain length of tail groups is extended (50). In contrast, our results showed that the chain length of spacers did not seem to affect the stability of ester linkages in the micelle core. The difference may be attributable to the fact that the mobility of spacers is restricted in the micelle core,

offsetting the effects of chain extension, whereas tail groups of prodrugs can move freely in solutions, leading to extended degradation half-lives of ester bonds. It is also possible that the surrounding micelle environment, including the hydrophilic PEG shell, might have attracted water molecules close to the ester linkages in polymer cores, and, therefore, hydrolysis reactions took place.

Tunable DEX Release from the Micelles

We analyzed the AUC of DEX release patterns to confirm tunable drug release from the micelles. Tunable drug release is important to control DEX distribution in tumors at different time points after the injection of polymer micelles. Tumor accumulation of polymer micelles was previously shown to reach its maximum level after 3 h post-injection (52). For this reason, the AUC values were analyzed both in the early (0–3 h) and late (3–24 h) stages of the drug release study (Fig. 4). Table I summarizes the results.

The AUC_{0-3} showed that ABA-M (45.20) effectively suppressed drug release at pH 7.4 with respect to EST-M (59.62). OHA-M (70.02) and OOA-M (83.86) released slightly more DEX than EST-M in the same period. At pH 5.0 (0–3 h), all micelles released DEX in a pH-dependent manner (ABA-M (105.38), OHA-M (76.27) and OOA-M (97.17)) compared to EST-M (30.29). At later time periods (AUC_{3-24}), DEX release at pH 7.4 was slower and more sustained in all dual-linker micelles compared to EST-M (1162.83): ABA-M (893.03), OHA-M (893.24), and OOA-M (983.39). The AUC_{3-24} at pH 5.0 showed that ABA-M (1536.74) released more DEX than either OHA-M (1106.28) or OOA-M (1254.63). It is interesting that OOA-M, containing longer and more hydrophobic spacers, released more DEX than OHA-M. Among the dual-linker micelles, ABA-M released the least drugs at pH 7.4 and the most drugs at pH 5.0 during the early time period (0–3 h). Using DEX release from ABA-M (100%) as the reference, release from OHA-M (155%) and OOA-M (186%) was greater at pH 7.4 between 0–3 h. OHA-M (72%) and OOA-M (92%) suppressed DEX release at pH 5.0 in the early period compared to ABA-M (100%). In the later time period (3–24 h), DEX release patterns at pH 7.4 were similar in all micelles (ABA-M (100%), OHA-M (100.0%) and OOA-M (110%)). At pH 5.0, however, ABA-M (100%) still released more DEX than OHA-M (72%) and OOA-M (82%).

These multi-step drug release profiles are desirable for achieving the necessary DEX concentrations at the tumor site. In the early stages following micelle accumulation in tumors, micelles are expected to exhibit a prompt drug release, bringing DEX concentrations up to the required level rapidly. The slower drug release at later time points

will allow for DEX concentration levels to be maintained over an extended period of time, reducing the need for multiple doses. It remains challenging for OHA-M and OOA-M to suppress DEX release at pH 7.4 while achieving tunable DEX release in acidic tumor environment. Based on these results, we considered ABA-M the optimal composition that would remain stable in blood and release DEX quickly in tumor tissues.

Enzymatic Stability of DEX-Loaded Micelles

Ester linkers can undergo enzymatic degradation in addition to hydrolysis. We tested stability of ABA-M in the presence of CE, a digestive enzyme of esters. We also investigated the influence of ions, small molecules (glucose, vitamins and amino acids), and proteins by testing stability of micelles in cell culture medium (RPMI) and FBS. Such investigation is of importance because the micelles will be exposed to various materials in the blood following injection. Instability in the presence of CE is critically important to be aware of because the CE activity of mouse plasma is significantly higher than human plasma, and studies performed in these animals may not give results representative of what would be observed in humans. Total drug release patterns (free DEX plus DEX-ABA) were compared at 0 and 24 h (Fig. 5). We observed no significant differences among the samples at the initial time point ($P > 0.05$). However, the micelles in mouse plasma containing CE showed a slight increase in DEX release at 24 h as compared to the RPMI control. Human plasma lacking CE activity caused no increase in DEX release. As $^1\text{H-NMR}$ of the micelles indicated that DEX was entrapped in the micelle core, it seemed unlikely that a 60–70 kDa CE enzyme could penetrate the micelle to this extent. However, this possibility cannot be excluded completely because no general protein destabilization effects on our polymer micelles were observed. Despite this, it is still reasonable to surmise that this minimal increase in DEX release (10–15% at 24 h) may not significantly impact the outcome of future *in vivo* studies using ABA-M. This apparent stability of polymer micelles in the presence of CE indicates that DEX-ABA should be primarily released in a pH-dependent manner at the tumor site followed by carboxylesterase-associated regeneration of free DEX.

CONCLUSION

In this study, we have shown that PEG-poly(aspartate) block copolymer micelles with hydrazone-ester dual linkers are a promising drug delivery platform for tunable release of DEX in tumors. In comparison to single hydrazone or ester linkers, hydrazone-ester dual linkers using ketonic acid

spacers are convenient and effective in changing the hydrophobicity of the micelle cores, chemical stability of drug conjugation linkages, and drug release patterns. The dual-linkers micelles appeared stable in the presence of CE, which can cause enzymatic degradation of ester bonds. Hydrazone-ester dual linkers may also be useful for other drug delivery platforms to achieve pH-dependent tunable drug release, especially for prodrugs that have been developed based only on ester chemistry. We envision that tunable drug release using hydrazone-ester dual linkers will bring a variety of options for combination chemotherapy and mixed drug delivery using polymer drug carriers in the pharmaceutical research area.

ACKNOWLEDGMENTS

Authors acknowledge financial support provided by the Kentucky Lung Cancer Research Program.

REFERENCES

- Duncan R. The dawning era of polymer therapeutics. *Nat Rev Drug Discov.* 2003;2:347–60.
- Putnam D, Kopecek J. Polymer conjugates with anticancer activity. *Adv Polym Sci.* 1995;122:55–123.
- Andresen TL, Thompson DH, Kaasgaard T. Enzyme-triggered nanomedicine: drug release strategies in cancer therapy. *Mol Membr Biol.* 2010;27(7):353–63.
- Lee ES, Gao Z, Bae YH. Recent progress in tumor pH targeting nanotechnology. *J Control Release.* 2008;132:164–70.
- Duncan R. Polymer conjugates as anticancer nanomedicines. *Nat Rev Cancer.* 2006;6:688–701.
- Oosterhoff D, Pinedo HM, van der Meulen IH, de Graaf M, Sone T, Kruyt FA, *et al.* Secreted and tumour targeted human carboxylesterase for activation of irinotecan. *Brit J Cancer.* 2002;87:659–64.
- Ponta A, Bae Y. PEG-poly(amino acid) block copolymer micelles for tunable drug release. *Pharm Res.* 2010;27(11):2330–42.
- West KR, Otto S. Reversible covalent chemistry in drug delivery. *Curr Drug Discov Technol.* 2005;2:123–60.
- Kratz F, Beyer U, Schutte MT. Drug-polymer conjugates containing acid-cleavable bonds. *Crit Rev Ther Drug.* 1999;16:245–88.
- Bae Y, Alani AWG, Rockich N, Lai TC, Kwon G. Mixed pH-sensitive polymeric micelles for combination drug delivery. *Pharm Res.* 2010;27(11):2421–32.
- Bae Y, Diezi TA, Zhao A, Kwon GS. Mixed polymeric micelles for combination cancer chemotherapy through the concurrent delivery of multiple chemotherapeutic agents. *J Control Release.* 2007;122:324–30.
- Hanahan D, Weinberg RA. The hallmarks of cancer. *Cell.* 2000;100:57–70.
- Scripture CD, Figg WD. Drug interactions in cancer therapy. *Nat Rev Cancer.* 2006;6:546–58.
- Smalley KSM, Haass NK, Brafford PA, Lioni M, Flaherty KT, Herlyn M. Multiple signaling pathways must be targeted to overcome drug resistance in cell lines derived from melanoma metastases. *Mol Cancer Ther.* 2006;5:1136–44.
- Atkins JH, Gershell LJ. Selective anticancer drugs. *Nat Rev Cancer.* 2002;2:645–6.
- Jain RK. Delivery of molecular and cellular medicine to solid tumors. *Adv Drug Del Rev.* 1997;26:71–90.
- Seymour LW, Duncan R, Strohalm J, Kopecek J. Effect of molecular weight (Mw) of N-(2-hydroxypropyl)methacrylamide copolymers on body distribution and rate of excretion after subcutaneous, intraperitoneal, and intravenous administration to rats. *J Biomed Mater Res.* 1987;21:1341–58.
- Hobbs SK, Monsky WL, Yuan F, Roberts WG, Griffith L, Torchilin VP, *et al.* Regulation of transport pathways in tumor vessels: Role of tumor type and microenvironment. *PNAS.* 1998;95(8):4607–12.
- Vander Heiden MG, Cantley LC, Thompson CB. Understanding the Warburg effect: the metabolic requirements of cell proliferation. *Science.* 2009;324:1029–33.
- Matsumura Y, Maeda H. A new concept for macromolecular therapeutics in cancer chemotherapy: mechanism of tumortropic accumulation of proteins and the antitumor agent SMANCS. *Cancer Res.* 1986;46:6387–92.
- Bae Y, Nishiyama N, Kataoka K. *In vivo* antitumor activity of the folate-conjugated pH-sensitive polymeric micelle selectively releasing adriamycin in the intracellular acidic compartments. *Bioconjugate Chem.* 2007;18:1131–9.
- Kano MR, Bae Y, Iwata C, Morishita Y, Yashiro M, Oka M, *et al.* Improvement of cancer-targeting therapy, using nanocarriers for intractable solid tumors by inhibition of TGF-beta signaling. *PNAS.* 2007;104:3460–5.
- Navaliltoha Y, Schwartz ES, Groothuis EN, Allen CV, Levy RM, Groothuis DR. Therapeutic implications of tumor interstitial fluid pressure in subcutaneous RG-2 tumors. *Neuro Oncol.* 2006;8:227–33.
- Kristjansen PEG, Boucher Y, Jain RK. Dexamethasone reduces the interstitial fluid pressure in a human colon adenocarcinoma xenografts. *Cancer Res.* 1993;53:4764–6.
- Wang H, Wang Y, Rayburn ER, Hill DL, Rinehart JJ, Zhang R. Dexamethasone as a chemosensitizer for breast cancer chemotherapy: potentiation of the antitumor activity of adriamycin, modulation of cytokine expression, and pharmacokinetics. *Int J Oncol.* 2007;30:947–53.
- Wang H, Li M, Rinehart JJ, Zhang R. Pretreatment with dexamethasone increases antitumor activity of carboplatin and gemcitabine in mice bearing human cancer xenografts: *in vivo* activity, pharmacokinetics, and clinical implications for cancer chemotherapy. *Clin Cancer Res.* 2004;10:1633–44.
- Franchimont D, Galon J, Gadina M, Visconti R, Zhou YJ, Aringer M, *et al.* Inhibition of Th1 immune response by glucocorticoids: dexamethasone selectively inhibits IL-12-induced Stat4 phosphorylation in T lymphocytes. *J Immunol.* 2000;164:1768–74.
- Auphan N, DiDonato JA, Rosette C, Helmberg A, Karin M. Immunosuppression by glucocorticoids: inhibition of NF- κ B activity through induction of I κ B synthesis. *Science.* 1995;270:286–90.
- Liu XM, Quan LD, Tian J, Alnouti Y, Fu K, Thiele GM, *et al.* Synthesis and evaluation of a well-defined HPMA copolymer-dexamethasone conjugate for effective treatment of rheumatoid arthritis. *Pharm Res.* 2008;25:2910–9.
- Wang D, Miller S, Liu XM, Anderson B, Wang XS, Goldring S. Novel dexamethasone-HPMA copolymer conjugate and its potential application in treatment of rheumatoid arthritis. *Arthritis Res Ther.* 2007;9(1):1–9.
- Krakovicova H, Etrych T, Ulbrich K. HPMA-based polymer conjugates with drug combination. *Eur J Pharm Sci.* 2009;37:405–12.
- Leopold CS, Friend DR. *In vitro* study drug for the assessment of poly(L-aspartic acid) as a drug carrier for colon-specific drug delivery. *Int J Pharm.* 1995;126:139–45.

33. Alani AWG, Bae Y, Rao DA, Kwon GS. Polymeric micelles for the pH-dependent controlled, continuous low dose release of paclitaxel. *Biomaterials*. 2010;31:1765–72.
34. Howard MD, Jay M, Dziubla TD, Lu X. PEGylation of nanocarrier drug delivery systems: state of the art, *J. Biomed Nanotechnol*. 2008;4(2):133–48.
35. Oyewumi MO, Yokel RA, Jay M, Coakley T, Mumper RJ. Comparison of cell uptake, biodistribution and tumor retention of folate-coated and PEG-coated gadolinium nanoparticles in tumor-bearing mice. *J Control Release*. 2004;95(3):613–26.
36. Takakura Y, Hashida M. Macromolecular carrier systems for targeted drug delivery: pharmacokinetic considerations on biodistribution. *Pharm Res*. 1996;13:820–31.
37. Yamaoka T, Tabata Y, Ikada Y. Distribution and tissue uptake of poly(ethylene glycol) with different molecular weights after intravenous administration to mice. *J Pharm Sci*. 1994;83:601–6.
38. Dreher MR, Liu W, Michelich CR, Dewhirst MW, Yuan F, Chilkoti A. Tumor vascular permeability, accumulation, and penetration of macromolecular drug carriers. *J Natl Cancer Inst*. 2006;98:335–44.
39. Kataoka K, Harada A, Nagasaki Y. Block copolymer micelles for drug delivery: design, characterization and biological significance. *Adv Drug Deliv Rev*. 2001;47:113–31.
40. Lian T, Ho RJY. Trends and developments in liposome drug delivery systems. *J Pharm Sci*. 2001;90:667–80.
41. Torchilin VP. Structure and design of polymeric surfactant-based drug delivery systems. *J Control Release*. 2001;73:137–72.
42. Matsumura Y, Kataoka K. Preclinical and clinical studies of anticancer agent-incorporating polymer micelles. *Cancer Sci*. 2009;100:572–9.
43. Bae Y, Kataoka K. Intelligent polymeric micelles from functional poly(ethylene glycol)-poly(amino acid) block copolymers. *Adv Drug Deliv Rev*. 2009;61:768–84.
44. Bae Y, Fukushima S, Harada A, Kataoka K. Design of environment-sensitive supramolecular assemblies for intracellular drug delivery: polymeric micelles that are responsive to intracellular pH change. *Angew Chem Int Ed*. 2003;42(38):4640–3.
45. Li B, Sedlacek M, Manoharan I, Boopathy R, Duysen EG, Masson P, et al. Butyrylcholinesterase, paraoxonase, and albumin esterase, but not carboxylesterase, are present in human plasma. *Biochem Pharmacol*. 2005;70:1673–84.
46. Kim MS, Cote CJ, Cristoloveanu C, Roth AG, Vornov P, Jennings MA, et al. There is no dose-escalation response to dexamethasone (0.0625–1.0 mg/kg) in pediatric tonsillectomy or adenotonsillectomy patients for preventing vomiting, reducing pain, shortening time to first liquid intake, or the incidence of voice change. *Anesth Analg*. 2007;104:1052–8.
47. Croy SR, Kwon GS. Polymeric micelles for drug delivery. *Curr Pharm Design*. 2006;12:4669–84.
48. Kale AA, Torchilin VP. Design, synthesis, and characterization of pH-sensitive PEG-PE conjugates for stimuli-sensitive pharmaceutical nanocarriers: the effect of substituents at the hydrazone linkage on the pH stability of PEG-PE conjugates. *Bioconjug Chem*. 2007;18:363–70.
49. Baker MA, Gray BD, Ohlsson-Wilhelm BM, Carpenter DC, Muirhead KA. Zyn-linked colchicines: controlled-release lipophilic prodrugs with enhanced antitumor efficacy. *J Controlled Release*. 1996;40:89–100.
50. Jordan CGM. How an increase in the carbon chain length of the ester moiety affects the stability of a homologous series of oxprenolol esters in the presence of biological enzymes. *J Pharm Sci*. 1998;87:880–5.
51. Yoshioka S, Stella VJ. *Stability of drugs and dosage forms*. New York: Kluwer Academic/Plenum Publishers; 2000.
52. Bae Y, Nishiyama N, Fukushima S, Koyama H, Matsumura Y, Kataoka K. Preparation and biological characterization of polymeric micelle drug carriers with intracellular pH-triggered drug release property: tumor permeability, controlled subcellular drug distribution, and enhanced *in vivo* antitumor efficacy. *Bioconjugate Chem*. 2005;16:122–30.